Biosensors and Bioelectronics 104 (2018) 87–94

Contents lists available at ScienceDirect

Biosensors and Bioelectronics

journal homepage: www.elsevier.com/locate/bios

Spore-based biosensor to monitor the microbicidal efficacy of gaseous hydrogen peroxide sterilization processes

Jan Oberländer[a,b], Marlena Mayer[c], Anton Greeff[c], Michael Keusgen[b], Michael J. Schöning[a,d,*]

[a] Institute of Nano-, and Biotechnologies (INB), Aachen University of Applied Sciences, Campus Jülich, Heinrich-Mußmann-Str.1, 52428 Jülich, Germany
[b] Institute of Pharmaceutical Chemistry, Philipps-University Marburg, Marbacher Weg 6-10, 35032 Marburg, Germany
[c] Elopak EQS GmbH, Hanns-Martin-Schleyer-Str. 17, 41199 Mönchengladbach, Germany
[d] Institute of Complex Systems 8 (ICS-8), Forschungszentrum Jülich GmbH, 52425 Jülich, Germany

ARTICLE INFO

Keywords:
Impedimetric biosensor
Microbiological spores
Sterilization process
Aseptic filling
Hydrogen peroxide (H_2O_2)

ABSTRACT

In this work, a spore-based biosensor is evaluated to monitor the microbicidal efficacy of sterilization processes applying gaseous hydrogen peroxide (H_2O_2). The sensor is based on interdigitated electrode structures (IDEs) that have been fabricated by means of thin-film technologies. Impedimetric measurements are applied to study the effect of sterilization process on spores of *Bacillus atrophaeus*. This resilient microorganism is commonly used in industry to proof the sterilization efficiency. The sensor measurements are accompanied by conventional microbiological challenge tests, as well as morphological characterizations with scanning electron microscopy (SEM) and transmission electron microscopy (TEM). The sensor measurements are correlated with the microbiological test routines. In both methods, namely the sensor-based and microbiological one, a tailing effect has been observed. The results are evaluated and discussed in a three-dimensional calibration plot demonstrating the sensor's suitability to enable a rapid process decision in terms of a successfully performed sterilization.

1. Introduction

Aseptic processing and filling of sensitive food products is a common technology for dairy products or juices. Main advantages of aseptic processing are the extended shelf life, the product distribution at ambient temperatures and protection of nutritional contents (Bockelmann and Bockelmann, 1998). One key process within this technology represents the sterilization of the packages to be filled with separately sterilized goods. In recent years, the package sterilization with vapor phase hydrogen peroxide (H_2O_2) at elevated gas temperature has been established (Ansari and Datta, 2003; Toledo, 1988). Hydrogen peroxide is known as a strong oxidizer and in combination with heat it possesses microbicidal and sporicidal activity (Toledo et al., 1973; Wallen, 1976). During the sterilization process at elevated temperature, H_2O_2 decomposes to oxygen and water vapor with intermediates of hydroxyl and hydroperoxyl radicals ($HO^{\bullet}$, $HO_2^{\bullet}$) and further reactive species of oxygen and hydrogen, such as O_2^{-}, $O^{\bullet}$ and $H^{\bullet}$ (McDonnell, 2009). Even though, the process of the lethal cell and spore damage is not clarified in detail yet, the generated radicals are proposed to be one of the species to be involved in deoxyribonucleic acid (DNA) damage of spores or bacteria (Cadet et al., 1999). In case of the more resilient spores, the protecting spore coat and membranes need first to be penetrated (Henriques and Moran, 2007; Leggett et al., 2015; Riesenman and Nicholson, 2000). The lethal damage of spores by applying H_2O_2 vapor at elevated temperature might be a combined process. In a first step, the molecules of the spore coat are oxidized and heat starts the degradation of proteins (Finnegan et al., 2010; Shintani et al., 2010). In a next step, the protection mechanism of the DNA, small, acid-soluble proteins bound to the spore DNA, needs to be deactivated by oxidation (McDonnell, 2007; Setlow and Setlow, 1993; Setlow, 2006). Finally, the DNA and thereby the reproduction system can be oxidized and damaged irreversibly.

The state-of-the-art methods to evaluate the performance and efficiency of package sterilization processes are laborious and time-consuming microbiological challenge tests (count-reduction test or end-point test) (Cerny, 1992; Food and Drug Administration, 2001; Verband Deutscher Maschinen- und Anlagenbau e.V. (VDMA), 2008). Numerous techniques have been applied to reduce the effort and workload of these challenge tests. Nutrition media with colorimetric pH indicators, for example, have been developed to enable a fast true/false detection of outgrowing microbiological colonies (Neogen Food Safety, 2017). A further method detects changes of the electrical properties of the growth medium; here, impedance measurements are performed on electrodes immersed into the medium. This technique can be

* Corresponding author at: Institute of Nano-, and Biotechnologies (INB), Aachen University of Applied Sciences, Campus Jülich, Heinrich-Mußmann-Str.1, 52428 Jülich, Germany.
E-mail address: schoening@fh-aachen.de (M.J. Schöning).

https://doi.org/10.1016/j.bios.2017.12.045
Received 19 October 2017; Received in revised form 15 December 2017; Accepted 26 December 2017
Available online 27 December 2017
0956-5663/

differentiated either as direct or indirect method. The direct method detects directly the metabolic activity of microorganisms by conductivity changes in the growth medium. Metabolic conversions of weakly or uncharged nutrition into highly charged end-products are increasing the media conductivity. For example, the conversion of non-ionized glucose into two molecules of lactic acid increases the media conductivity (Silley and Forsythe, 1996). The indirect method monitors the metabolic carbon dioxide (CO_2) production of the microorganisms. The impedance electrodes are immersed into a potassium hydroxide (KOH) solution, which is in a sealed environment together with the culture medium. The increasing CO_2 concentration results in a conductance decrease of the KOH solution (Owens et al., 1989). Both impedimetric detection methods are available in commercial cell analysis systems such as: BacTrac®, SY-Lab GmbH; R.A.B.I.T.®, Don Whitley Scientific Ltd.; Bactometer®, Vitek Systems, Malthus®, Malthus Instruments Ltd. etc. (Cady et al., 1978). However, they are not able to monitor alterations on the spore morphology and the resulting spore death, induced by sterilization processes.

A first step into this direction was a recently introduced by an impedimetric sensor to directly monitor the sterilization efficiency by means of detecting the degradation of bacterial spores (Oberländer et al., 2015a, 2015b). This sensor is based on interdigitated electrode structures (IDEs) on which resilient microbiological organisms are immobilized, comparable to conventional challenge tests. Sensors based on interdigitated electrodes are commonly used to monitor chemical or biochemical processes in liquids. Examples are given in Bianchi et al. (2012), Couniot et al. (2015), Gerwen et al. (1998) and Lisdat and Schafer (2008). Those sensitive electrode structures have also been implemented in gaseous detection systems as well as for particle monitoring in air as described e.g., in Blue and Uttamchandani (2017), Carminati et al. (2014), Weiss et al. (2015) and York et al. (2001). In the present work, detailed studies on the development of a spore-based impedimetric biosensor system will be presented and discussed. Especially, investigations of the sensor signal behavior with regard to the sterilization parameters are in focus to implement a parametric calibration matrix describing the sterilization efficacy.

2. Materials and methods

2.1. Spore suspension, microbiological evaluation

The spore suspension was based on a strain of *Bacillus atrophaeus* (DSM 675) purchased from IVV Fraunhofer, Germany. The preparations of the spore suspension, as well as the sensor functionalization and microbiological reference tests, were performed aseptically under a laminar flow work bench. The spore suspensions were prepared and purified as explained previously (Arreola et al., 2017). The purified spore suspensions were diluted in deionized (DI) water and stored at 4 °C. The load of the microbial spore suspension was adjusted to a colony count of 1×10^9 cfu/ml (cfu: colony forming unit). As reference test either the sensor chip itself or sample substrates of glass were investigated with microbiological challenging tests (as industrially applied). The sensors and glass samples were inoculated with an aliquot of 10 µl of spore suspension to achieve a final load of 1×10^7 cfu, which corresponds to conventional microbiological tests in industry. After sterilization process with gaseous hydrogen peroxide, the spores were recovered and resuspended in Ringer's solution with 0.01% Tween 80 as surfactant combined with ultrasonic treatment for 10 min. The enumeration of the surviving colonies was performed by serial dilutions of the resulting suspensions and spread-plated on plate-count agar (PCA). After incubation time of 5 days at 30 °C the outgrown colonies could be counted. The logarithmic cycle reduction (LCR, see Eq. (1)) was determined by the initial number of spores per sample (N_0) and the number of outgrown colonies (N) after the sterilization process. The number of outgrown colonies was calculated by a weighted mean in accordance to Adams and Moss (2008) and Verband Deutscher Maschinen- und Anlagenbau e.V. (VDMA) (2008).

$$\mathrm{LCR} = \log(N_0/N) \quad (1)$$

2.2. Sensor fabrication

The investigated sensors were in-house fabricated by means of thin-film technologies. The fabrication procedure is schematically depicted in the Supplementary information Fig. S1. As substrate a Borofloat® glass wafer (Schott GmbH) was chosen with a thickness of 500 µm, which possesses reduced parasitic capacitances compared to conventional silicon wafers with necessary insulation layers. Electron beam evaporation was used to deposit the electrode materials (first layer: 10 nm chromium; second layer: 100 nm gold) on top of the glass wafers. Chromium was used as an adhesion promoter between glass and gold. The subsequent electrode pattern was transferred photolithographically into a spin-coated negative photoresist layer (AZ nLOF 2020, Merck KGaA). For that, a customized chromium glass mask with interdigitated electrodes was applied. The width and interspacing of the electrodes are designed to be 3 µm and 7 µm, respectively, each electrode finger has a length of 3.25 mm; a total number of 614 fingers captures an area of approximately 20 mm^2. The photoresist layer serves as an etching-mask for the following reactive ion-etching process (RIE, Plasmalab 100, Oxford Inc.). A gas mixture of argon at 10 sccm and oxygen at 15 sccm has been applied to transfer the electrode pattern into the metal layers. To finalize the RIE process the photoresist mask has been removed by oxygen plasma treatment. A further lithography process was applied to develop SU-8 walls to enable a defined immobilization of the spore suspension. The final wafer was then diced into single sensor chips of 5×10 mm^2 (a sensor chip without SU-8 walls is shown exemplarily in Fig. 1b).

2.3. Sensor characterization

The sensor fabrication, as well as, the microbiological spores have been evaluated by means of scanning electron microscopy (SEM) on a Jeol JSM-7800F. The spores were additionally characterized by transmission electron microscopy (TEM) on a Zeiss Libra® 120.

The developed sensors were electrically investigated by impedance measurements. For all measurements the sensors were placed into a customized measurement chamber as shown in Fig. 1a. The measurement chamber enables the defined connection of the single sensors. Moreover, to maintain a comparable measurement environment (humidity, temperature, pressure) a vacuum pump (Laboport N 86kN.18, KNF Neuberger GmbH) was connected during the measurements, adjusting a pressure of 100 mbar (absolute) within the chamber. Gold-covered spring contacts were applied to guarantee a reproducible sensor connection. The spring contacts were connected externally to an Agilent precision LCR-Meter (E4980 A). The excitation voltage was set to 20 mV with a 0 V DC (direct current) bias. The impedance sweeps were performed in a frequency range between 200 Hz and 200 kHz. Detailed sensor evaluations were performed at a fixed frequency of 3 kHz. Four independent sensors were measured after each step of handling: first, measurement was performed of the blank IDE structures; second, after the immobilization of the spore suspension or drying of pure, deionized (DI) water as reference on the IDE surface; and finally, after the sterilization process with gaseous H_2O_2.

2.4. Sterilization process

In this work, all sterilization processes were carried out on a sterilization test rig that is already described in Kirchner et al. (2011) and Näther et al. (2006). The process is adapted to the sterilization processes of industrial aseptic filling machines applying gaseous hydrogen peroxide. The test rig uses pressurized air as carrier gas, which is controlled by a flow meter and regulation valve. Two piston pumps are

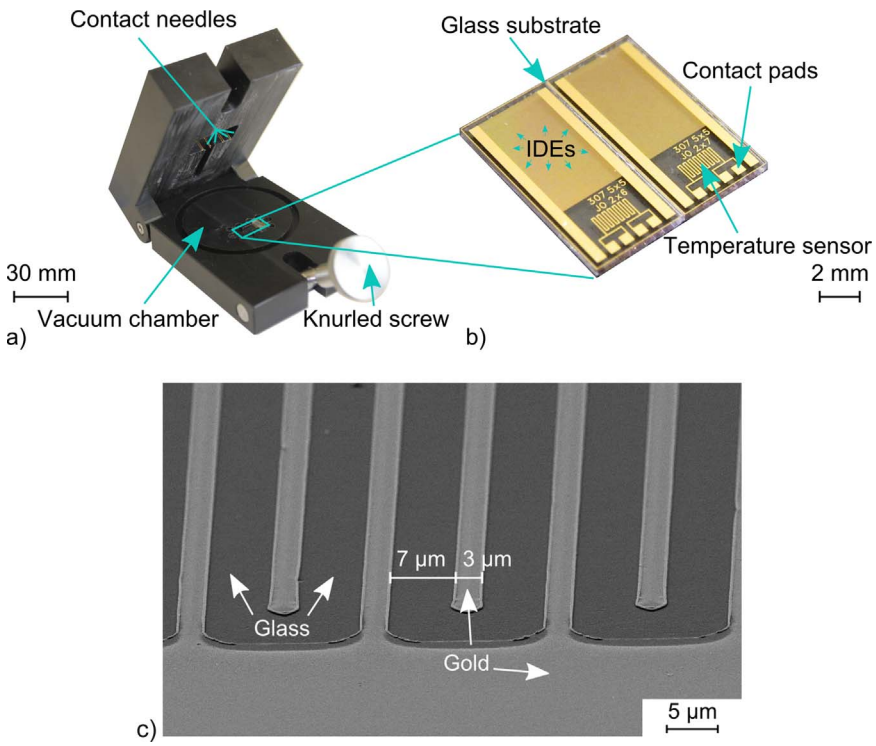

Fig. 1. Characterization set-up to evaluate the sterilization process by means of the developed biosensor: (a) vacuum measurement chamber; (b) differential set-up of two glass-based interdigitated electrodes (IDEs) and temperature sensors, serving as biosensor chip. (c) SEM picture of the developed IDE gold structures. Side walls on the electrodes can be recognized caused by the RIE process.

used as dosage systems for H_2O_2 solution (Interox® 35% w/w, Solvay S.A.) and for DI water; both media are fed into the carrier gas and can be controlled independently. An evaporation unit consisting of two heating elements is used to transfer the mixture into the gas phase. The power of the heating elements is controlled by the medium temperature at the evaporation unit outlet. The sensors and microbiological samples are exposed to the sterilization processes via a time-controlled hydraulic slide in a defined distance to the gas nozzle of the test rig, comparable to industrial sterilization processes of composite packages.

The process parameters are chosen according to actual decontamination cycles of aseptic composite packages for liquid food. The gas temperature has been adjusted to 240 °C at a constant air flow of 10 m^3/h. Different sterilization scenarios have been investigated by varying the H_2O_2 concentration between 0% v/v and 8.3% v/v. The present H_2O_2 concentration has been logged in addition with one of our previously developed calorimetric H_2O_2 gas sensors (Kirchner et al., 2012, 2013; Oberländer et al., 2015c). The calorimetric gas sensor consists of a differential set-up of a catalytically active and a passive temperature sensor. The exothermal decomposition of H_2O_2 correlates with the present H_2O_2 concentration. The exposure times of the sensors and microbiological samples are given in the results section.

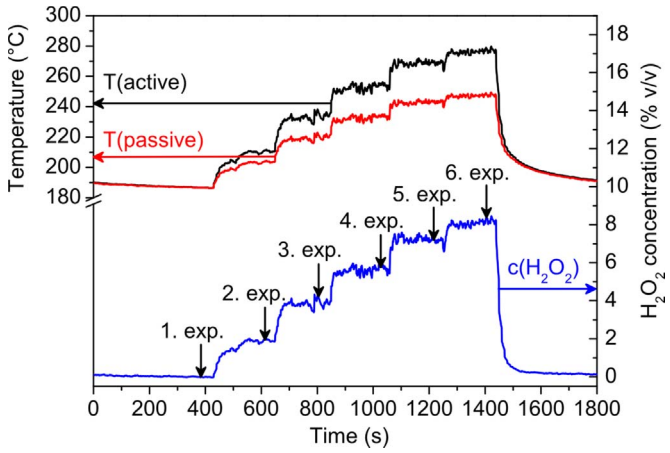

Fig. 2. Signal response of the calorimetric H_2O_2 gas sensor, to determine the prevailing H_2O_2 concentration during the subsequent biosensor and sample exposure. The upper part depicts the temperature plots of the calorimetric sensor set-up, one catalytically activated and one passivated. The lower part depicts the resulting H_2O_2 concentration and times of sensor/sample exposures (1. exp. to 6. exp.).

3. Results and discussion

During the sterilization process, the H_2O_2 concentration has been monitored by an additional calorimetric gas sensor. The corresponding measurement plot is shown in Fig. 2, where the exposure moments of the biosensor/microbiological samples are indicated, too (see 1. exp. to 6. exp.). The upper part of the diagram represents the temperatures of the catalytically activated (catalyst Pt on Al_2O_3) and the passivated temperature sensor. The resulting H_2O_2 concentration is given in the lower part, determined by the temperature difference of the differential set-up with a sensor's sensitivity of 3.58 °C/(% v/v H_2O_2).

3.1. Microbiological kill rate study

As a reference tool to the biosensor-based evaluation (see Section 3.3), microbiological kill rate studies during the sterilization process were performed. The recovery rate of three non-sterilized samples, per run was used to determine the initial load of the microbiological samples, i.e. the glass substrate and sensor chips, respectively (Fig. 3a), whereby an average value of $9.8 \times 10^6 \pm 4.6$ cfu/sample could be obtained. The load number is slightly lower as given in Section 2.1, which can be related to the applied recovery process: not all spores were re-suspended into the solution, remaining spores have been observed on the samples. Nonetheless, the recovery rate can be determined to 98%, that represents an excellent value. The resulting average number has been taken into account to calculate the logarithmic cycle reduction (LCR) for the following experiments.

In order to determine the dependency between the LCR and the present H_2O_2 concentration, in a first set of experiments the exposure time was varied between 0.2 s and 0.5 s (Fig. 3b). A correlation

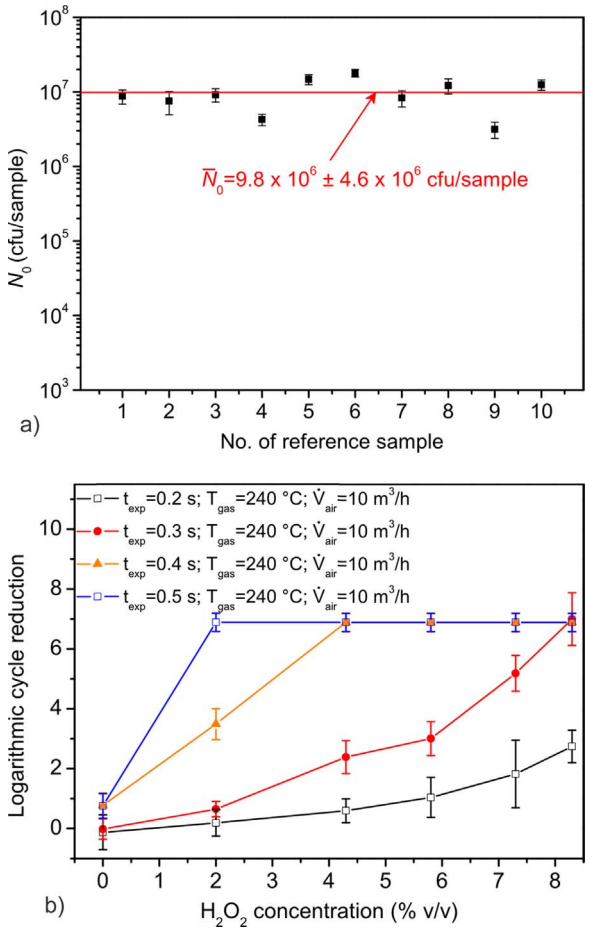

Fig. 3. (a) Evaluation of the number of microorganisms recovered from reference samples. (b) Logarithmic cycle reduction for different exposure times (between 0.2 s and 0.5 s) with varying concentrations (0–8.3% v/v) of gaseous H_2O_2.

between the process at different H_2O_2 concentrations and the LCR can be observed for all exposure times. For short exposure times of 0.2 s, however, a kill rate (logarithmic cycle reduction) of maximum 2.7 is reached, which not fulfills industrial standards (this should be ideally 6 or higher). On the other hand, for exposure times of 0.4 s and 0.5 s, the linear relation between increasing H_2O_2 concentration and logarithmic cycle reduction is only valid for H_2O_2 concentrations up to 4.3% v/v and 2% v/v, respectively. Thereby, to have a linear relationship in the whole H_2O_2 concentration range of interest, an exposure time of 0.3 s has been selected for the further experiments, which will also allow the correlation with the biosensor-based evaluation.

3.2. Sensor characterization

Beside the electrical characterization of the sensors the IDE structures were analyzed by SEM. As shown in Fig. 1c, a repetitive pattern of the gold electrodes was produced by use of RIE. The parameters of the electrodes have been analyzed to 3 µm in width and an interspacing width of 7 µm, as predefined by the applied lithography mask. The SEM images further exhibit the topography of the electrodes, which have a slightly elevated side wall. This phenomenon is related to redeposited etching products during the RIE process. The redeposition during the RIE process has been also described by other groups (Aydemir and Akin, 2012; Franz et al., 2002). To overcome this issue the gas constituents and the masking layer should be further adjusted in future experiments. Nonetheless, compared with our previous work, where the lift-off method for electrode patterning was applied (Oberländer et al., 2015a), the electrode structure now depicts defined edges. This results

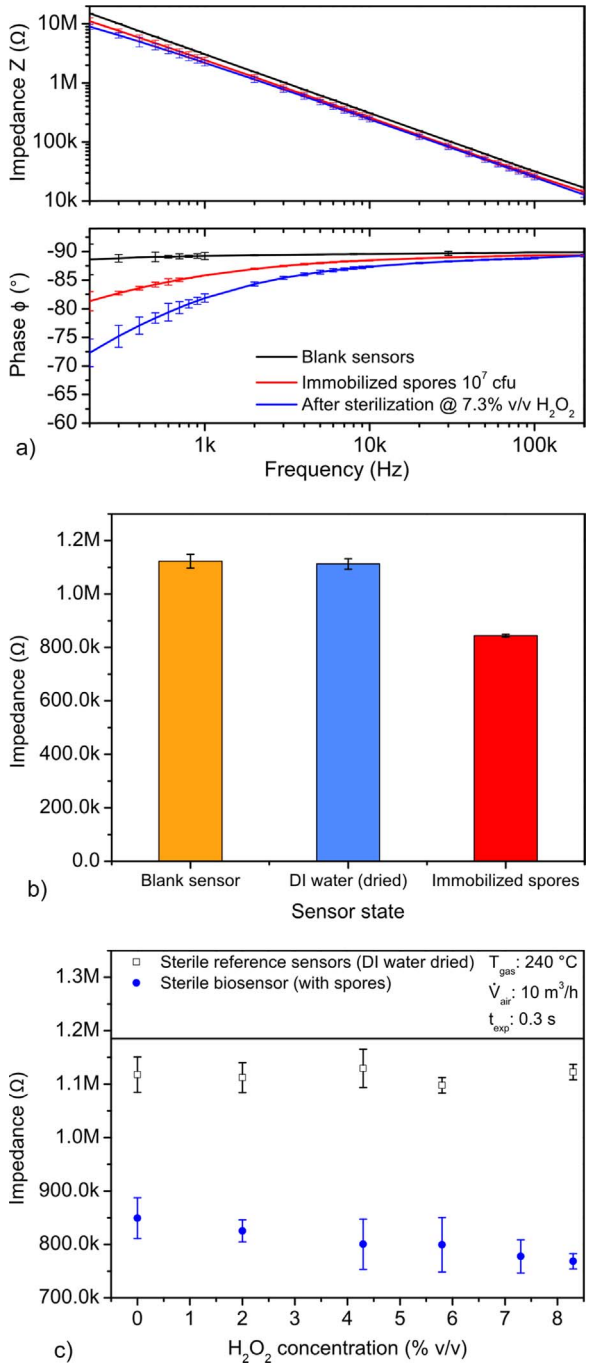

Fig. 4. (a) Impedimetric biosensor characterizations, Bode plot of biosensor measurements at different states: black line represents mean values of four blank sensor structures; red line corresponds to mean values of four sensors after immobilization of 10^7 cfu; blue line represents mean values of four sensors after sterilization for 0.3 s at 7.3% v/v, temperature 240 °C, air flow 10 m^3/h. (b) Mean impedance values measured at a frequency of 3 kHz: impedance values of non-sterilized IDE, blank sensors (orange bar, number of sensors N = 48); 10 µl DI water dried as reference (blue bar, N = 24); with immobilized spores, 10^7 cfu per IDE structure (red bar, N = 24). (c) Impedance values after sterilization, exposure time 0.3 s: reference sensors (DI water dried) (black open squares, N = 4 for each concentration); sterilized biosensor with spores (blue dots, N = 4 for each concentration). (For interpretation of the references to color in this figure legend, the reader is referred to the web version of this article.)

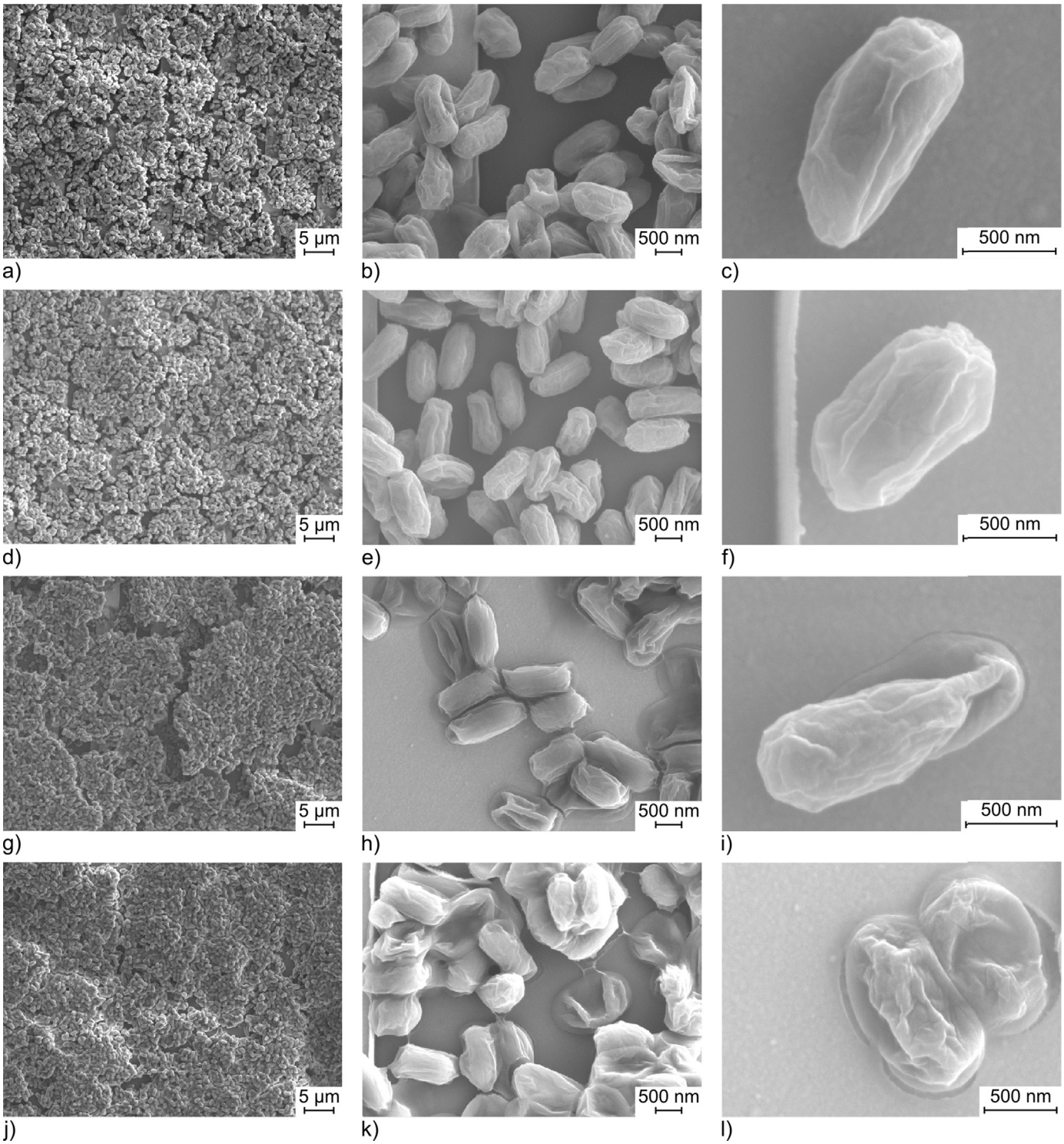

Fig. 5. Scanning electron microscopy pictures of spore layers before and after sterilization treatment: (a)–(c) spore reference no treatment; (d)–(f) after hot air treatment 0.3 s; (g)–(i) after sterilization 0.3 s at 4.3% v/v H_2O_2; (j)–(l) after sterilization 0.3 s at 8.3% v/v H_2O_2; gas parameter: temperature 240 °C, air flow 10 m^3/h.

in a more homogenous distribution of the electric field for the impedimetric measurements (see Section 3.3).

3.3. Biosensor-based evaluation

For each measurement the impedance spectra were recorded in a frequency range between 200 Hz and 200 kHz. The impedance average plot of four sensors is shown in the Bode diagram in Fig. 4a. The first impedance plot was captured from bare IDE structures (Fig. 4a), upper plot, black line, Z(f = 3 kHz) = 1.12 MΩ). As the measurements were performed in a vacuum atmosphere a strict capacitive behavior can be determined over the whole frequency range, with a phase of about −90° (Fig. 4a, lower plot, black line). After immobilizing and drying of the microbiological spores an impedance decrease can be monitored (Fig. 4a, upper plot, red line, Z(f = 3 kHz) = 844 kΩ). At low frequencies (200 Hz–10 kHz) the phase shows more conductive behavior, corresponding to the spore layer and the change in permittivity compared to the blank sensor (Fig. 4a, lower plot, red line). A further

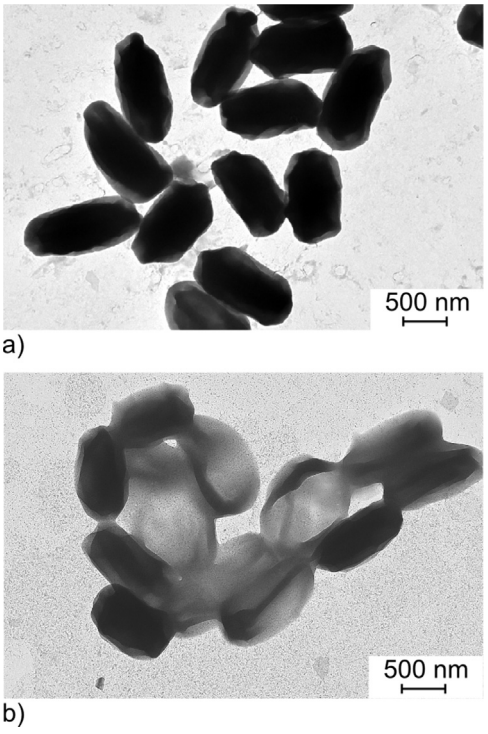

Fig. 6. Transmission electron microscopy pictures of spores: (a) spore reference, no treatment; (b) after sterilization 0.3 s at 8.3% v/v H_2O_2, temperature 240 °C, air flow 10 m^3/h.

impedance decrease can be monitored after the sterilization process (Fig. 4a, upper plot, blue line, Z(f = 3 kHz) = 777 kΩ). This impedance change is related to morphological alterations, such as degradation and rupture of the spores, caused by the sterilization process. The conductivity increase can be explained by the flattened spore structure after sterilization, which enhances the current flow between the electrodes. Furthermore, an additional layer has been formed after the sterilization process, which might be attributed to the release of inner spore substances.

To validate these assumptions and to reveal the morphological effects of the sterilization process and sensing mechanism, surface analyzes were applied after different sterilization scenarios using SEM (Fig. 5). It should be declared, some of the effects observed by SEM are related to the characterization at vacuum (10^{-5} Pa) e.g., the shrunken structure. In a comparison between non-treated and treated spores a significant difference can be observed when comparing Fig. 5c, f, i, and l. Non-treated or heat-treated spores show a denser and elliptical structure as spores after sterilization. Even though, also on the reference images already some deformed spores could be found, which could be related to the preparation of the spore suspension. The morphology change after the sterilization could also be seen in transmission electron microscopy studies (s. Fig. 6). Furthermore, after the sterilization process some of the spores ruptured and collapsed (Fig. 5k, l, Fig. 6b). Additionally, a layer between the spores and the electrodes could be observed (Fig. 5k); similar rupture effects have also been reported after plasma treatment (Deng et al., 2006). Both facts are directly related to an enhancement of the conductivity between the electrodes, which leads to a decrease in the impedance signal as achieved in the impedance plot in Fig. 4a.

In order to study the impact of the H_2O_2 concentration toward the sensor signal further impedance investigations were performed. The resulting sensor signal was analyzed at a fixed frequency of 3 kHz. In a first step, the results of the reference sensors (blank sensors and after DI water drying, without spores) will be discussed. The mean impedance value of all blank sensors used in this work (N = 48) is evaluated to

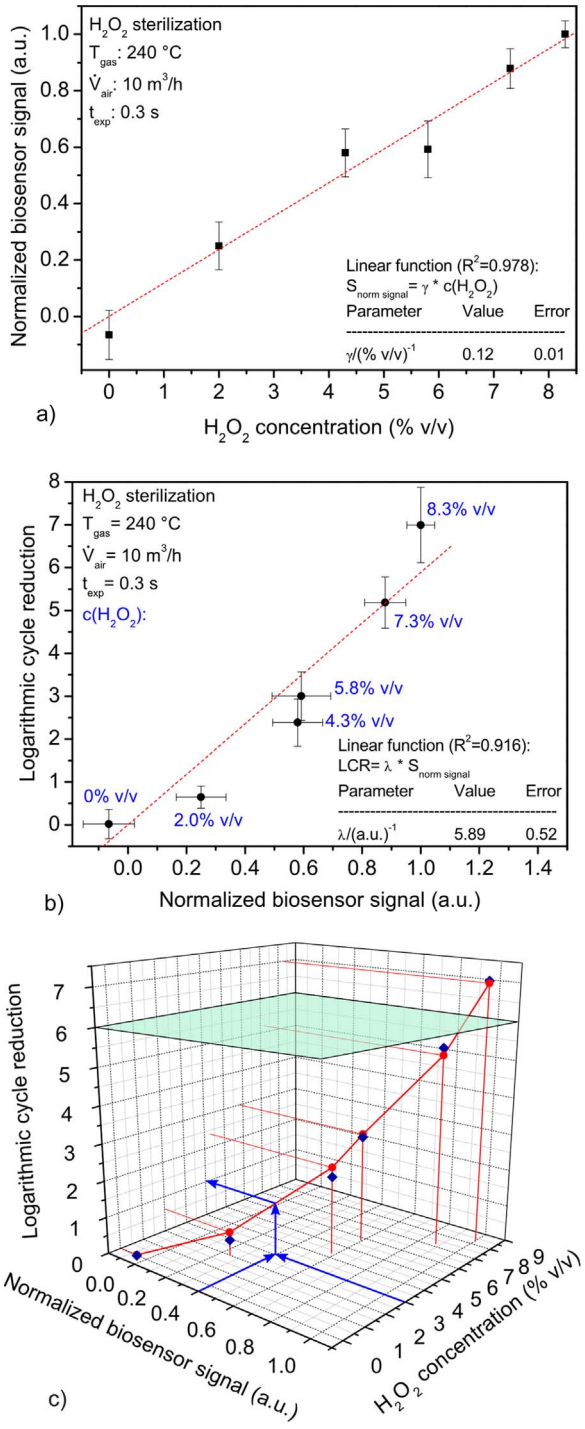

Fig. 7. Correlations between parameters of the H_2O_2 sterilization process: (a) plot of the normalized biosensor signal vs. the measured H_2O_2 concentration; (b) logarithmic cycle reduction vs. normalized biosensor signal. (c) Parametric, three-dimensional calibration plot: normalized biosensor signal (lower left axis) and measured H_2O_2 concentration (lower right axis) enable a prediction of the resulting logarithmic cycle reduction (vertical axis) (measured values, red dots). The green plane depicts the required LCR value for aseptic packaging. As a control of the derived LCR function (Eq. (5)) the resulting values are plotted as blue squares. Blue arrows indicate the graphical method to predict the LCR value by using the resulting value of the biosensor signal and the measured H_2O_2 concentration by the calorimetric gas sensor. (For interpretation of the references to color in this figure legend, the reader is referred to the web version of this article.)

(1.12 ± 0.26) MΩ (Fig. 4b orange bar). After drying of 10 µl DI water on the reference sensors (N = 24) a mean impedance value of (1.11 ± 0.19) MΩ has been recorded (Fig. 4b blue bar), which is very

Table 1
Comparison between the standardized, microbiological evaluation method and the biosensor-based method to evaluate the sterilization efficacy.

Microbiological method	Biosensor-based method
+ Standardized and accepted method (FDA, VDMA)	+ Fast evaluation < 1 h
- Final result evaluation after 72 h	+ Electrical read-out signal
- Lab- and time-consuming method	+ In-field application, next to the filling machine
- Costly method	+ Cost reduction, no nutrition medium etc.
- Experienced laboratory personnel necessary	+ Easy application by trained engineers
- High sample number, due to fluctuations of microbiological results	- Non-standardized method until now

FDA: Food and Drug Administration, USA; VDMA: Verband Deutscher Maschinen- und Anlagenbau e.V., Germany.

close to that of the blank sensors. The reference sensors were also exposed to the harsh environment of the sterilization process, in order to proof their stability and possible drift effects. Four independent sensors have been chosen for each H_2O_2 concentration. The measured impedance results versus the particular H_2O_2 concentration are shown in (Fig. 4c black open squares). The plot reveals small deviations between different sensors, indicated by the error bars and only slight fluctuations of the sensors for different H_2O_2 concentrations. Overall, these characterizations proof that no interactions between the harsh sterilization process and the IDE structure occurs, which ensures the further measured effects are related to the spore layer on top of the sensors.

In Fig. 4b, the mean impedance values, after functionalizing the sensors with a spore layer are evaluated to (844.4 ± 5.2) kΩ (red bar, N = 24). The small standard deviation (error bar) depicts a reproducible spore immobilization on top of the sensors.

Again, four independent sensors have been chosen for each H_2O_2 concentration. Compared to the mean value before, a further impedance decrease can be monitored (Fig. 4c blue, filled dots). Moreover, the impedance decrease is in relation to the present H_2O_2 concentration and thereby to the sterilization efficiency. In order to compare the resulting differences, the normalized sensor signal as difference between the signals of immobilized spores (Z_{spores}) and after their sterilization ($Z_{sterile}$) has been calculated using Eq. (2):

$$\text{Normalized sensor signal} = (Z_{spores} - Z_{sterile})/Z_{spores} \quad (2)$$

These normalized results of the spore-based biosensor have been combined with the measured H_2O_2 concentrations, presented in Fig. 7a. Overall, a linear relation between the normalized biosensor signal and the present H_2O_2 concentration can be found, see Eq. (3) ($R^2 = 0.978$).

$$S_{norm\ signal} = 0.12(\%v/v)^{-1}\cdot c(H_2O_2) \quad (3)$$

Here, $S_{norm\ signal}$ represents the normalized biosensor signal and c (H_2O_2) denotes the present H_2O_2 concentration.

A signal stagnancy-type behavior can be observed between H_2O_2 concentrations of 4.3% and 5.8% v/v, which might be related to partially non-injured spores after the sterilization process. A similar effect has been observed during the performed microbiological reference tests (Fig. 3b) LCR plot (red line)). In literature, this stagnancy effect has been discussed as tailing effect, which can be related to stacked spore layers at the sample/sensor surfaces, as also observed in our experiments Fig. 5a, d, g, j (Warriner et al., 2000).

In Fig. 7b, the LCR values of the performed microbiological reference tests have been plotted versus the normalized sensor signals, yielding again a linear relationship. The linear function between the normalized biosensor signal and the LCR values allows a prediction of the sterilization efficiency by the electrical sensor read-out of the biosensor, see Eq. (4) ($R^2 = 0.916$).

$$LCR = 5.89(\text{a. u.})^{-1}\cdot S_{norm\ signal} \quad (4)$$

Both sensing methods, biosensor set-up and calorimetric H_2O_2 detection, are combined with the LCR values in a three-dimensional parametric calibration plot (Fig. 7c). A calibration function has been evaluated to Eq. (5) ($R^2 = 0.769$).

$$LCR = 0.85(\%v/v)^{-1}\cdot S_{norm\ signal}\cdot c(H_2O_2) \quad (5)$$

The combination of both independent sensing principles enables a rapid process evaluation. The resulting biosensor signal and the measured H_2O_2 concentration can be combined with Eq. (5), whereby the resulting LCR value is calculated or graphically evaluated as shown in Fig. 7c. The efficacy of the sterilization process can be quantified within 15 min, compared to the conventional, microbiological method, which takes 48 h up to one week until final evaluation. This fast process evaluation leads to an enormous reduction in time and workload, especially, during the parameterization of new sterilization systems or testing different process settings (e.g., gas concentration, air flow). Moreover, an in-field process control would be possible, without extended product storage during incubation of microbiological samples.

4. Conclusion

An impedimetric, spore-based biosensor has been introduced to facilitate a rapid control and parameterization of gaseous sterilization processes. The impedimetric measurements were combined with microbiological logarithmic cycle reduction tests. For the first time, the impedimetric biosensor has been applied at different H_2O_2 concentrations, depicting a relation between the logarithmic cycle reduction and the H_2O_2 concentration. Both characterizations, the conventional microbiological test routine as well as the biosensor set-up, have shown a tailing effect between 4.3% v/v and 5.8% v/v H_2O_2. Additionally, surface characterizations of the IDE structure, as well as of the microbiological spores at different H_2O_2 concentrations were performed. This study revealed information about the morphological changes of the spores, whereby sensing principles have been proposed. Table 1 summarizes the advantages and drawbacks of the conventional microbiological and the biosensor-based method, respectively.

In further studies, different sterilization scenarios will be investigated, such as variations in air flow and temperature. In future experiments, the biosensor can be implemented in industrial filling machines, as well as food packages. This might enable a fast process control during initial operation tests, after maintenance or as in-field process control, which will reduce the laborious microbiological challenge tests, improve product safety and minimize product recalls.

Acknowledgments

The project was financially supported by the Federal Ministry of Education and Research, Germany, Project: “ImpediPack” (Fund. No.: 03FH012I3). Prof. Dr. J. Bongaerts is acknowledged for offering the lab equipment to run the microbiology studies, H. Iken for assisting the sensor fabrication, D. Rolka for the SEM characterizations, and C. Zafiu for the TEM characterizations, C. Hansen for supporting the sensor measurements.

Appendix A. Supplementary material

Supplementary data associated with this article can be found in the online version at http://dx.doi.org/10.1016/j.bios.2017.12.045.

References

Adams, M.R., Moss, M.O. (Eds.), 2008. Food Microbiology, 3rd ed. Royal Society of Chemistry, Cambridge, UK.
Ansari, I.A., Datta, A.K., 2003. Food Bioprod. Process. 81 (1), 57–65.
Arreola, J., Oberländer, J., Mätzkow, M., Keusgen, M., Schöning, M.J., 2017. Electrochim.

Acta 241, 237–243.
Aydemir, A., Akin, T., 2012. J. Micromech. Microeng. 22 (7), 74004–74009.
Bianchi, E., Rollo, E., Kilchenmann, S., Bellati, F.M., Accastelli, E., Guiducci, C., 2012. Detecting particles flowing through interdigitated 3D microelectrodes. In: Proceedings of Annual International Conference of the IEEE Engineering in Medicine and Biology Society (EMBC), 2012. San Diego, California, USA, Aug. 28 - Sept. 1, 2012. IEEE, Piscataway, NJ, pp. 5002–5005.
Blue, R., Uttamchandani, D., 2017. Meas. Sci. Technol. 28 (2), 22001–22024.
Bockelmann, B.A.H., von, Bockelmann, I.L.I. von, 1998. Long-Life Products. Heat-Treated, Aseptically Packed: A Guide to Quality. B. von Bockelmann, Åkarp, Sweden.
Cadet, J., Delatour, T., Douki, T., Gasparutto, D., Pouget, J.-P., Ravanat, J.-L., Sauvaigo, S., 1999. Mutat. Res. 424 (1–2), 9–21.
Cady, P., Dufour, S.W., Shaw, J., Kraeger, S.J., 1978. J. Clin. Microbiol. 7 (3), 265–272.
Carminati, M., Pedalà, L., Bianchi, E., Nason, F., Dubini, G., Cortelezzi, L., Ferrari, G., Sampietro, M., 2014. Sens. Actuators, A 219, 80–87.
Cerny, G., 1992. Packag. Technol. Sci. 5 (2), 77–81.
Couniot, N., Afzalian, A., Overstraeten-Schlögel, N., van, Francis, L.A., Flandre, D., 2015. Sens. Actuators, B 211, 428–438.
Deng, X., Shi, J., Kong, M.G., 2006. IEEE Trans. Plasma Sci. 34 (4), 1310–1316.
Finnegan, M., Linley, E., Denyer, S.P., McDonnell, G., Simons, C., Maillard, J.Y., 2010. J. Antimicrob. Chemother. 65 (10), 2108–2115.
Food and Drug Administration, 2001. Guide to Inspections of Aseptic Processing and Packaging for the Food Industry.
Franz, G., Kachel, R., Sotier, S., 2002. Mat. Sci. Semicon. Proc. 5 (1), 45–50.
Gerwen, P., van, Laureyn, W., Laureys, W., Huyberechts, G., Beeck, M. op de, Baert, K., Suls, J., Sansen, W., Jacobs, P., Hermans, L., Mertens, R., 1998. Sens. Actuators, B 49 (1–2), 73–80.
Henriques, A.O., Moran, C.P., 2007. Annu. Rev. Microbiol. 61, 555–588.
Kirchner, P., Li, B., Spelthahn, H., Henkel, H., Schneider, A., Friedrich, P., Kolstad, J., Keusgen, M., Schöning, M.J., 2011. Sens. Actuators, B 154 (2), 257–263.
Kirchner, P., Oberländer, J., Friedrich, P., Berger, J., Rysstad, G., Keusgen, M., Schöning, M.J., 2012. Sens. Actuators, B 170, 60–66.
Kirchner, P., Oberländer, J., Suso, H.-P., Rysstad, G., Keusgen, M., Schöning, M.J., 2013. Food Control 31 (2), 530–538.
Leggett, M.J., Schwarz, J.S., Burke, P.A., McDonnell, G., Denyer, S.P., Maillard, J.-Y., 2015. Appl. Environ. Microbiol. 82 (4), 1035–1039.
Lisdat, F., Schafer, D., 2008. Anal. Bioanal. Chem. 391 (5), 1555–1567.
McDonnell, G., 2007. Peroxygens and other forms of oxygen: their use for effective cleaning, disinfection, and sterilization. In: Zhu, P.C. (Ed.), New Biocides Development. The Combined Approach of Chemistry and Microbiology. American Chemical Society, Washington, D.C, USA, pp. 292–308.
McDonnell, G., 2009. The use of hydrogen peroxide for disinfection and sterilization applications. In: Rappoport, Z. (Ed.), PATAI'S Chemistry of Functional Groups. John Wiley & Sons, Ltd, Chichester, UK, pp. 1–34.
Näther, N., Juárez, L.M., Emmerich, R., Berger, J., Friedrich, P., Schöning, M.J., 2006. Sensors 6 (4), 308–317.
Neogen Food Safety, 2017. National food laboratory aseptic validation medium, product information. 〈www.neogen.com〉 (accessed 12 September 2017).
Oberländer, J., Bromm, A., Wendeler, L., Iken, H., Durán, M.P., Greeff, A., Kirchner, P., Keusgen, M., Schöning, M.J., 2015a. Phys. Status Solidi A 212 (6), 1299–1305.
Oberländer, J., Jildeh, Z.B., Kirchner, P., Wendeler, L., Bromm, A., Iken, H., Wagner, P.H., Keusgen, M., Schöning, M.J., 2015b. Sensors 15 (10), 26115–26127.
Oberländer, J., Kirchner, P., Keusgen, M., Schöning, M.J., 2015c. Electrochim. Acta 183, 130–136.
Owens, J.D., Thomas, D.S., Thompson, P.S., Timmerman, W., 1989. Lett. Appl. Microbiol. 9 (6), 245–249.
Riesenman, P.J., Nicholson, W.L., 2000. Appl. Environ. Microbiol. 66 (2), 620–626.
Setlow, B., Setlow, P., 1993. Appl. Environ. Microbiol. 59 (10), 3418–3423.
Setlow, P., 2006. J. Appl. Microbiol. 101 (3), 514–525.
Shintani, H., Sakudo, A., Burke, P., McDonnell, G., 2010. Exp. Ther. Med. 1 (5), 731–738.
Silley, P., Forsythe, S., 1996. J. Appl. Bacteriol. 80 (3), 233–243.
Toledo, R.T., 1988. Overview of sterilization methods for aseptic packaging materials. In: Hotchkiss, J.H. (Ed.), Food and Packaging Interactions: Developed from a Symposium Sponsored by the Division of Agricultural and Food Chemistry at the 193rd Meeting of the American Chemical Society, Denver, Colorado, April 5–10, 1987. American Chemical Society, Washington, DC, USA, pp. 94–105.
Toledo, R.T., Escher, F.E., Ayres, J.C., 1973. Appl. Microbiol. 26 (4), 592–597.
Verband Deutscher Maschinen- und Anlagenbau e.V. (VDMA), 2008. VDMA-Fachverbandsschriften 6, 1–16.
Wallen, S.E., 1976. Sporicidal action of hydrogen peroxide. Wallen, S.E., 1976. Sporicidal action of hydrogen peroxide. Ph.D. Thesis, Ames, IA, USA., Ames, IA, USA.
Warriner, K., Rysstad, G., Murden, A., Rumsby, P., Thomas, D., Waites, W.M., 2000. J. Appl. Microbiol. 88 (4), 678–685.
Weiss, A., Bauer, M., Eichenauer, S., Stadlbauer, E.A., Kohl, C.-D., 2015. J. Sens. Sens. Syst. 4 (1), 37–44.
York, T.A., Evans, I.G., Pokusevski, Z., Dyakowski, T., 2001. Sens. Actuators, A 92 (1–3), 74–79.